JOURNAL OF MATERIALS SCIENCE 22 (1987) 1913–1918

Cellular intergrowth between quartz and sodium-rich plagioclase (myrmekite) – an analogue of discontinuous precipitation in metal alloys

R. WIRTH
Institut für Werkstofftechnologie Fachbereich 12.1 Bau 2, Universität Saarbrücken, 6600 Saarbrücken, FRG
G. VOLL
Mineralogisches Institut der Universität zu Köln, Zülpicherstr.49, 5000 Köln 1, FRG

Gneissic rocks of the contact aureole of the Traversella Intrusion (N. Italy) reveal a cellular intergrowth of quartz and oligoclase (myrmekite), originating from alkali feldspar grain boundaries. The myrmekite occurs in a temperature range of 500 to 670° C. The size of the cells and the lamellar spacing of the quartz rods increase with rising temperature. A comparison of the characteristic features of myrmekite cells with discontinuous precipitation cells of alloys indicates many similarities between the reactions. It is concluded that the formation of myrmekite is a solid-state reaction; a supersaturated alkali feldspar decomposes into a cellular structure growing behind a moving incoherent grain boundary. Micro probe analyses of the original alkali feldspar, the reaction products, and the volume relationship of the reactants (quartz, sodium-rich plagioclase) show that an ion exchange occurs during the reaction (K^+ removed; Na^+, Ca^{2+} and Si^{4+} added). A model describing the early stages of the formation of myrmekite is presented.

1. Introduction

The feldspars are the most important mineral group in the upper lithosphere. The majority of feldspars may be classified chemically as members of the ternary system $NaAlSi_3O_8$ (albite)–$KAlSi_3O_8$ (alkali feldspar)–$CaAl_2Si_2O_8$ (anorthite). Members of the series between $NaAlSi_3O_8$ and $KAlSi_3O_8$ are called alkali feldspars, and those between $NaAlSi_3O_8$ and $CaAl_2Si_2O_8$ plagioclase feldspars [1]. A supersaturated alkali feldspar reduces its free energy by phase separation into sodium-rich and potassium-rich components. Alkali feldspars can adjust their composition easily by diffusion of potassium and sodium (and calcium) in the solid state. Three different mechanisms of precipitation are possible [2]:

(i) The alkali feldspar precipitates oriented lamellae by nucleation and growth or by spinodal decomposition.

(ii) Rims of albite (or orthoclase) are formed at the grain boundaries of alkali feldspars by heterogeneous nucleation of albite [3].

(iii) Myrmekite, a cellular intergrowth of quartz and sodium-rich plagioclase, is nucleated at the grain boundary [2].

Myrmekite is an intergrowth between quartz and sodium-rich plagioclase that is situated next to alkali feldspar. Myrmekite may be found as blebs between adjacent but differently oriented alkali feldspar crystals. This type is called intergranular myrmekite [4]. Myrmekite may be found in minor or accessory amounts in any plutonic rock which contains quartz and perthitic alkali feldspar (two-phase alkali feldspar). The following characteristic properties are attributed to myrmekite in the literature:

(i) It is always associated with alkali feldspar [5].

(ii) The plagioclase of the myrmekite cell is commonly a sodium-rich plagioclase (oligoclase). There may be a proportional relationship between the volume of quartz and the anorthite component of the associated myrmekite plagioclase [4].

(iii) If the overall surface of the intergrowth is bulbous or nodular and convex towards associated potash feldspar, then the quartz rods may fan out and describe crude radii within the host plagioclase. The quartz rods tend to stand approximately normal to the surface [4, 6] (Fig. 1).

(iv) The quartz rods tend to maintain a definite mean lateral spacing as a function of the temperature of formation. Very often, the quartz rods terminate abruptly in blunt lobes, usually at the presumed original alkali feldspar grain boundary [4, 7].

(v) The plagioclase in myrmekite is crystallographically parallel to the primary alkali feldspar on which it forms a rim. In cases where myrmekite is set as a series of double blebs between two adjacent alkali feldspar crystals (intergranular myrmekite), the orientation of the plagioclase of one set of blebs is the same as that of the perthitic

0022–2461/87 $03.00 + .12

plagioclase in the potash feldspar to which it is attached [3, 6].

(vi) Myrmekite only occurs at migrating, high-angle grain boundaries [6, 8].

(vii) Myrmekite formation occurs only during cooling [7].

A discontinuous precipitation reaction of an alloy (cellular reaction) is a solid-state phase transformation which results in the decomposition of a supersaturated solid solution into a cellular structure consisting of two (or more) stable phases. In many systems, the decomposition involves the migration of an incoherent interface (reaction front) between the supersaturated solid solution and the cellular structure. The decomposition occurs predominantly by an interfacial diffusion process from the solid solution to the corresponding phases in the cellular structure. The incoherent interface (reaction front) is usually formed by the migration of a high-angle grain boundary which was present in the supersaturated solid solution [9]. The discontinuous precipitation reaction is reviewed by Hillert [10] and Hornbogen [11].

The driving force for the movement of the incoherent grain boundary in discontinuous precipitation is the difference in free energy between the supersaturated solid solution and its equilibrium phases. The precipitates of the discontinuous precipitation cells show a lamellar arrangement. The width of the lamellae and the lamellar spacing are controlled by the interfacial energy of the lamellae and the grain-boundary diffusion coefficient. That is, the lamellar spacing and the width of the lamellae depend on the temperature of the discontinuous precipitation reaction [12].

A comparison of the characteristic features of myrmekite formation with those of discontinuous cellular precipitation in metal alloys shows many features in common. It is the main purpose of the present paper to show that myrmekites are formed in a similar way to discontinuous cellular precipitates in metal alloys. An example of myrmekite formation in the contact aureole (the area around an intrusion, affected by the heat of an intrusion) of a magmatic intrusion is given. A summation reaction scheme for the formation of myrmekites is deduced, and a model describing the early stages of the myrmekite formation is presented. The geological setting and the distribution of the maximum temperatures in the contact aureole as a function of the distance from the intrusion are described elsewhere [13].

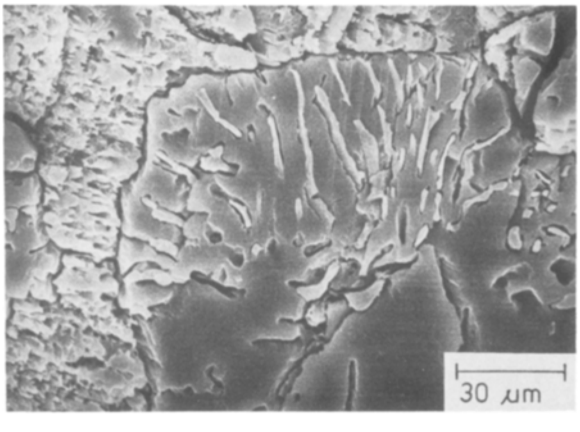

Figure 1 SEM micrograph showing a myrmekite cell growing into an alkali feldspar (characterized by etch pits). The bright rods are quartz in a matrix of sodium-rich plagioclase (oligoclase). The original grain boundary between the two adjacent alkali feldspars runs NE–SW, and is decorated with lobes of quartz (sample was etched with hydrofluoric acid).

2. Experimental details and methods

For polarized light analysis of myrmekite, thin sections were cut from suitable rock samples. For qualitative investigations with a scanning electron microscope (SEM) (Cambridge Stereoscan 180, fitted with an energy dispersive EDAX system), samples were etched with hydrofluoric acid. Chemical analyses were carried out on polished thin sections with an ARL microprobe using standard material for reference (Sanidine 751 for potassium; albite Amelia County for silicon, aluminium and sodium; anorthite glass An-100 for calcium).

Samples for transmission electron microscopy (TEM) studies were prepared from uncovered thin sections. Suitable areas were selected with the polarizing microscope and marked. These areas were extracted from the thin sections by means of Technovit 5071 (Technovit 5071 is a cold-curing resin for indirect surface testing and impressions). Technovit protects the sample from damage during the extraction and can be removed from the sample by acetone. The samples, mounted on copper grids (diameter 3 mm), were thinned for TEM by ion beam milling (argon 99.999; 5 kV, 80 mA), and coated with carbon. TEM was performed at 200 kV in a JEOL JEM 200A with side-entry goniometer.

Quartz and oligoclase volumes were calculated from optical photomicrograph enlargements of about 15 myrmekite cells using the line sectioning method described in detail elsewhere [14]. The size of the myrmekite cells was measured by means of light microscopy, using a calibrated ocular. The diameters of about 50 different myrmekite cells per thin section were measured parallel and normal to the reaction front, and the mean values were calculated. For measuring the spacing of the quartz rods the same method was used.

3. Results

3.1. Microscopic observations

In gneissic rocks (crystalline schists with quartz, feldspar and mica as major components) within the contact aureole of the Traversella Intrusion (quartz–diorite–monzonite), alkali feldspars with considerable amounts of myrmekite can be found. The maximum temperature at the contact depends on the temperature of the intrusion, the depth of the intrusion, the temperature of the country rocks at that depth, and is estimated to be 640 to 670° C [13]. With increasing distance from the intrusion, the maximum temperature within the contact aureole decreases to 500 to 520° C at about 80 m (the temperatures are deduced from the breakdown reaction of phengite, and the occurrence of microcline–sanidine) [13]. This is the temperature interval in which myrmekite is

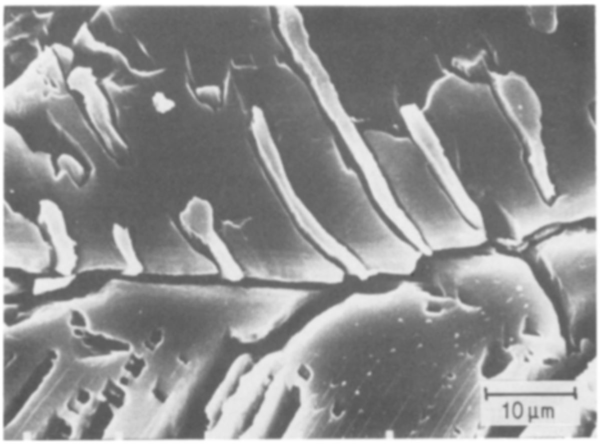

Figure 2 SEM micrograph of myrmekite with a cellular arrangement of quartz in a sodium-rich plagioclase matrix (oligoclase). The reaction front is marked by the terminating quartz rods. The lower part of the micrograph shows the partially replaced alkali feldspar. The thin, parallel, NE–SW bright lines in the alkali feldspar are oriented exsolution lamellae of albite.

observed in the contact aureole of the Traversella Intrusion.

Polarized light analyses of thin sections of suitable rock samples reveal that, originating from alkali feldspar grain boundaries and occasionally from plagioclase/alkali feldspar phase boundaries, alkali feldspar is replaced by a cellular arrangement of quartz and sodium-rich plagioclase (oligoclase) (Fig. 2). Alkali feldspar is never completely replaced by myrmekite cells, and twin boundaries in alkali feldspar do not nucleate myrmekite cells. This is consistent with the observations of Schreyer and of Voll [6, 8]. Additionally, there is precipitation of thin albite lamellae ($< 1\,\mu m$) within the alkali feldspars (Fig. 3). This type of precipitation is already described in the literature [2].

The quartz rods are approximately normal to the boundary between myrmekite and alkali feldspar. The average cell dimensions (mean values of the dimension vertical and parallel to the reaction front) and the lateral spacing of the quartz rods increase towards the contact (Table I). The oligoclase of the myrmekite cells and the alkali feldspar with which it shares a common grain boundary have the same crystallographic orientation. In the sample shown in Fig. 4 two alkali feldspars (I, II) have a common grain boundary. The oligoclase of the myrmekite cell growing into the alkali feldspar II then adopts the crystallographic orientation of alkali feldspar I. Similar behaviour has been observed by Smith in metal alloys, and by Voll in silicates [6, 15].

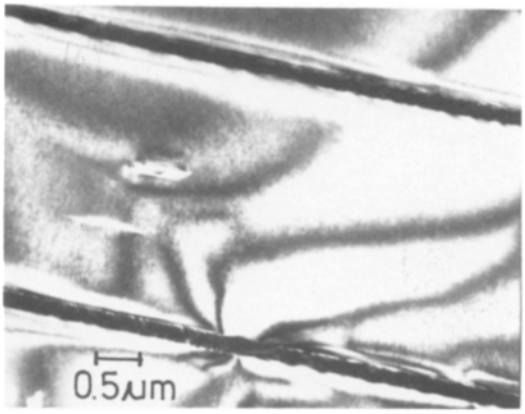

Figure 3 Parallel exsolution lamellae of albite in alkali feldspar. TEM micrograph, bright field image.

3.2. Chemistry

Traverses of electron microprobe analyses across myrmekite cells and the adjacent alkali feldspars show that the plagioclase of the myrmekite cells is oligoclase (plagioclase with about 2.3 wt % CaO). The results of the analyses are shown in Table II. These traverses indicate a remarkable decrease in K_2O in the alkali feldspar compared with the plagioclase from approximately 13 wt % to 0.3 wt %. However, the Na_2O content increases from 2 wt % in the alkali feldspars to 10.5 wt % in oligoclase. There is a sodium-depleted zone in the alkali feldspar in the vicinity of the alkali feldspar/oligoclase phase boundaries. Na_2O decreases from about 1.5 wt % to 0.5 to 1.0 wt % as the boundary is approached (Fig. 5). At the boundary, the Na_2O content increases dramatically. Comparing the chemical analyses of the starting material (alkali feldspar) and of the myrmekite (oligoclase, quartz), it is evident that ion transport is involved with the formation of myrmekite.

Considering the volume of the quartz rods and the volume of oligoclase in the myrmekite cells, and comparing these volume relationships with theoretical predictions, a discrepancy becomes obvious. From the chemical composition (wt %) and the density of the minerals involved [1], the amount of the different oxides within a definite volume ($1\,cm^3$) can be calculated. The basic assumption for this calculation is the postulated immobility of aluminium during metamorphic reactions [16], i.e. the Al_2O_3 content of the alkali feldspar–myrmekite system is assumed to be constant. A volume of $1\,cm^3$ of alkali feldspar contains 0.49 g Al_2O_3. However, $1\,cm^3$ oligoclase contains 0.56 g Al_2O_3. Consequently, without additional Al_2O_3, $1\,cm^3$ alkali feldspar can only be replaced by $0.87\,cm^3$ oligoclase. The replacement of alkali feldspar by

TABLE I Increasing cell dimensions and increasing rod spacing of quartz as a function of distance from the intrusion

Temperature (° C)	Distance (m)	Cell dimension (µm)	Rod spacing of quartz (µm)
~ 580	41	48	4.5
	24	56	4.8
	17	52	6.2
	12	62	7.0
	8	62	7.4
	4	67	6.4
~ 660	1	65	6.9

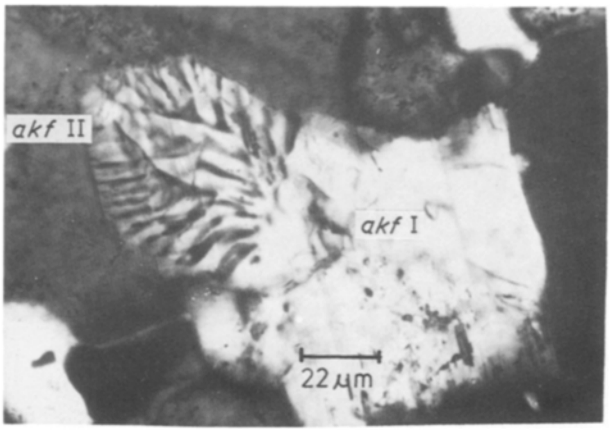

Figure 4 Optical micrograph of a myrmekite cell growing into alkali feldspar II (crossed polars). The bright areas inside the myrmekite cell (oligoclase) and the bright alkali feldspar I indicate an identical crystallographic orientation relationship between oligoclase and alkali feldspar I.

myrmekite needs an alkali ion exchange and a supply of CaO (see Table III). The replacement of 1 cm^3 alkali feldspar by 0.87 cm^3 oligoclase also creates 0.16 g SiO_2. However, this amount of quartz only fills a volume of 0.06 cm^3, i.e. 6 vol % in contrast to the 14 to 24 vol % quartz seen microscopically in the myrmekite cells. The discrepancy between this observation and the calculation suggest that SiO_2 was also added to the system.

4. Discussion

There are strong analogies between myrmekites from the contact aureole of the Traversella Intrusion and cellular (discontinuous) precipitates in metals. The formation of myrmekite is a nucleation and growth process which is associated with a moving, incoherent boundary. The identical crystallographic orientation of oligoclase in the myrmekite cell with one of the original alkali feldspars forming the grain boundary is an indication of cellular reaction.

The mobility of grain boundaries depends on the relative crystallographic orientation of the neighbouring grains [17]. Twin boundaries are immobile compared with other high-angle grain boundaries, and a strong driving force is necessary to displace them. Normally, in alloys, no discontinuous precipitation cells occur at twin boundaries. The reaction free energy (the driving force) is not sufficient. However, an additional driving force – stored deformation energy – acting on the twin boundary results in a moving grain boundary, thus creating discontinuous precipitation cells [9].

The thickness of the rods of cellular precipitation and the rod spacing is related to the annealing temperature. Thickness and rod spacing are optimized by the system in such a way that the lateral diffusion path in the grain boundary and the interfacial energy between the precipitates tend to a minimum [12]. The quartz rods in the myrmekites show the same behaviour, as previously pointed out by Voll [7].

However, there is one important point in which the formation of myrmekite deviates from the discontinuous precipitation reaction. The replacement of alkali feldspar by myrmekite (oligoclase + quartz) involves mass transport. During the formation of myrmekite cells material is added and another material is removed from the system by diffusion. K^+ is removed, Ca^{2+}, Na^+ and Si^{4+} are added to the system. There are two different possible sources for these elements. One is the intrusion itself: the liquid phase of an intrusion penetrates the rocks of the contact aureole. There is strong evidence for such a penetration. The transfer of material from the magma to the country rocks has generated diopside and garnet skarns (calc–silicate rocks in connection with ore deposits of contact metamorphic origin) [18]. During contact metamorphism in the contact aureole, minerals like phengite (mica) and glaucophane (amphibole) are replaced by other minerals [13, 19]. These reactions result in a surplus of ions like Na^+ and Ca^{2+} which can interact with the minerals of the surrounding rocks. Sodium for the formation of oligoclase comes partially from the albite component of the alkali feldspars. However, the analyses indicate that this is not sufficient, and Na^+ must have been added by diffusion.

Assuming the creation of myrmekite cells by a solid-state reaction associated with a moving, incoherent grain boundary, we have to consider the driving force for the reaction and the boundary movement. With decreasing temperature, the supersaturated alkali

TABLE II Microprobe analysis (weight %)

Alkali feldspar																
CaO	0.01	0.01	0.03	0.01	–	0.01	0.19	0.04	0.04	0.06	0.14	0.07	0.01	0.01	0.01	0.01
Na_2O	3.1	2.7	2.9	2.1	1.9	2.0	3.8	1.8	2.2	1.6	2.6	1.6	2.9	1.9	1.7	1.4
K_2O	12.3	12.6	12.3	13.3	13.4	13.2	10.7	13.5	13.2	13.6	12.6	13.8	12.4	13.5	13.6	13.9
Al_2O_3	18.9	18.5	18.9	18.6	18.8	18.9	19.0	18.9	19.0	18.9	18.9	18.9	18.9	18.6	18.5	18.7
SiO_2	64.5	63.8	64.1	63.3	64.2	64.1	63.8	63.9	64.0	63.9	63.9	63.7	64.2	63.0	63.5	63.3
Total	98.8	97.6	98.3	97.3	98.3	98.2	97.5	98.1	98.4	98.1	98.1	98.1	98.4	97.0	97.3	97.3
Oligoclase from myrmekite cells																
CaO	2.4	2.2	2.3	2.2	2.3	2.3	2.1									
Na_2O	10.4	10.4	10.4	10.3	10.4	10.3	10.4									
K_2O	0.3	0.3	0.4	0.3	0.3	0.3	0.3									
Al_2O_3	21.7	21.3	21.6	21.1	21.4	21.5	21.3									
SiO_2	65.7	66.6	65.3	66.5	65.3	65.4	65.8									
Other	11.9	10.9	11.4	10.9	11.4	11.4	10.5									
Total*	100.5	100.8	100.0	100.4	99.7	99.8	99.9									

*Includes the un-named components.

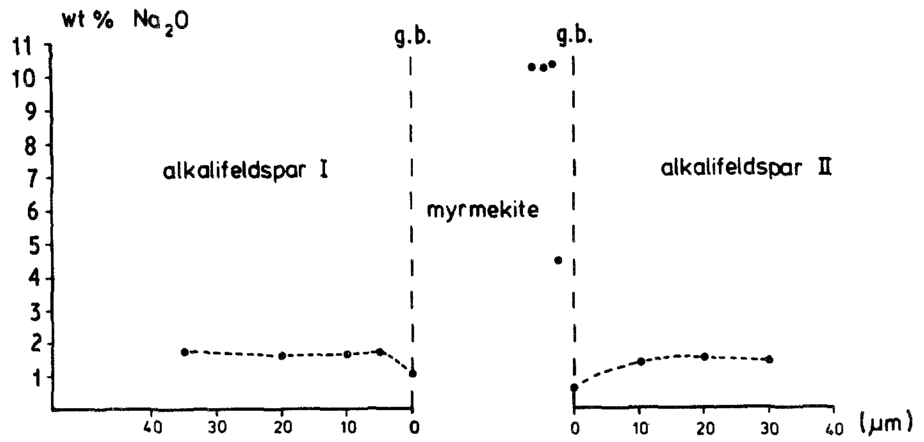

Figure 5 Graph showing the depletion of Na_2O in the vicinity of the grain boundary alkali feldspar/myrmekite (oligoclase).

feldspar reduces its free energy by precipitating its albite component. As pointed out above, there are three different ways of achieving this more favourable state:

(i) Precipitation of oriented lamellae of albite

(ii) Formation of rims of albite at the grain boundaries

(iii) Formation of myrmekite.

The formation of myrmekite cells only occurs if Ca^{2+} ions are available in the grain boundary. The Na_2O-depleted zone in the alkali feldspar just in front of the grain boundary, and the very steep increase of the Na_2O content just behind the boundary indicates diffusion of sodium into the grain boundary. Similar behaviour was observed in Cu–5 wt % Ag alloys [9]. The early stage of discontinuous precipitation in these alloys is characterized by grain-boundary precipitates in a stationary grain boundary, resulting in a silver-depleted zone in the vicinity of the grain boundary. The silver-depleted zone is indicated by the lack of silver-rich precipitates in the vicinity of the grain boundary. The boundary itself is decorated with larger grain-boundary silver-rich precipitates.

Very often, these grain-boundary precipitates mark the original grain boundary in precipitation cells. In myrmekite cells, quartz blebs mark the original boundary.

Oligoclase nucleates at suitable nucleation sites in the alkali feldspar grain boundary, depending on the crystallographic orientation of the neighbouring grains and the inclination of the boundary plane. Thin sections reveal that the crystallographic orientation of the oligoclase is the same as one of the alkali feldspars. The result is that this interface has a lower boundary energy than the crystallographically misoriented interface oligoclase–alkali feldspar I (Fig. 6). The difference in the interfacial energies results in a driving force on the grain boundary, thus initiating a movement of the grain boundary. The moving grain boundary envelopes the grain-boundary precipitates (oligoclase), replacing the interface with the higher energy by one with a lower energy. This mechanism is very similar to the Tu and Turnbull mechanism which describes the early stage of discontinuous precipitation in Pb–Sn alloys [20]. The grain boundary with the boundary precipitates starts moving despite a narrow, depleted zone in the vicinity of the grain boundary (reduced driving force). Once moving, the grain boundary leaves the depleted area and approaches the supersaturated crystal. Then an additional driving force, the reaction free energy, acts on the grain boundary. Behind the moving grain boundary, a cellular arrangement of oligoclase and quartz is established.

Concurrently with the formation of the myrmekite cells, albite precipitates as thin, oriented lamellae in the alkali feldspar. Due to the precipitation of albite inside the alkali feldspar, the driving force for the boundary movement involved with the formation of myrmekite decreases, and the cellular reaction ceases. This is consistent with the observation that, in the samples reported here, alkali feldspar is never totally replaced by myrmekite cells. Myrmekites only occur at the margins of alkali feldspars. In the formation of myrmekite an "open" system is involved, as pointed out above. Spencer [21] rejects an "open" system, since he finds it hard to understand why myrmekite cells form at the grain boundary. Myrmekite should be created continuously at all grain boundaries where a fluid phase with Na^+ and Ca^{2+} ions is present. However, considering the formation of myrmekite cells as analogous to discontinuous precipitation in

TABLE III Comparison of the chemical composition of alkali feldspar and oligoclase of the myrmekite cell

	Alkali feldspar (ϱ = 2.56 g cm^{-3})		Oligoclase (ϱ = 2.63 g cm^{-3})		Oligoclase	
	wt %	g in 1 cm^3	wt %	g in 1 cm^3	wt %	g in 0.87 cm^3
SiO_2	65.1	1.67	65.8	1.73	65.8	1.51
Al_2O_3	19.2	**0.49**	21.4	0.56	21.4	**0.49**
K_2O	13.3	0.34	0.3	0.01	0.3	0.01
Na_2O	2.35	0.06	10.4	0.27	10.4	0.24
CaO	0.04	1.02×10^{-3}	2.2	0.06	2.2	0.05
Total	99.99	2.56	100.1	2.63	100.1	2.30

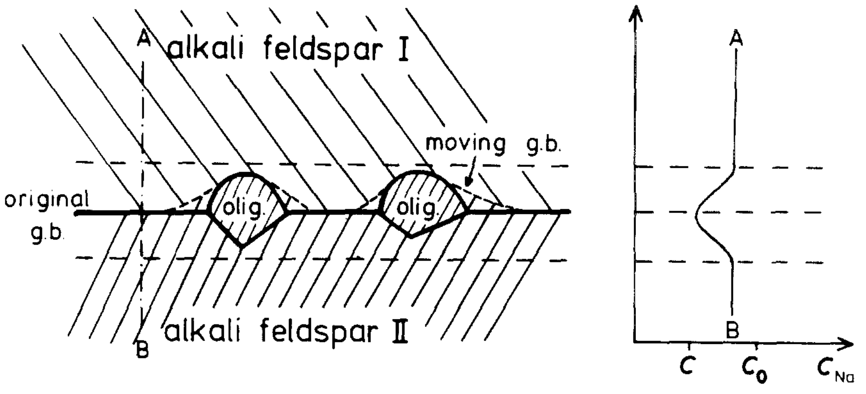

Figure 6 Schematic presentation of the early stage of the formation of myrmekite cells. The common crystallographic orientation of the grain-boundary precipitates (oligoclase) and alkali feldspar II is indicated by parallel lines with different spacing. The dashed lines on either sides of the original grain boundary mark the Na_2O-depleted zone. The sodium concentration profile on the right corresponds to the travers A–B.

alloys, the existence of dispersed nucleation sites at the grain boundary is reduced to a nucleation problem.

Acknowledgements

The authors would like to thank Professor Dr K. Jasmund and especially Dipl. Min H. Höfer for critically reading the manuscript. The financial support of the Deutsche Forschungsgemeinschaft through grant Wirth (Wi-662/1-5) is gratefully acknowledged.

References

1. W. A. DEER, R. A. HOWIE and J. ZUSSMAN, in "Rock-forming minerals", Vol. 4, (Longman, London, 1963) p. 1.
2. L. WIDENFALK, *Lithos* **2** (1969) 295.
3. H. RAMBERG, *Neues Jahrb. Miner. Abh.* **98** (1962) 14.
4. E. R. PHILLIPS, *Lithos* **7** (1974) 181.
5. F. K. DRESCHER-KADEN, *Mineralogie und Petrographie in Einzeldarstellungen* **1** (1948) 1.
6. G. VOLL, *Liverpool and Manchester Geol. J.* **2** (1960) 503.
7. G. VOLL, *Fortschritte Mineralogie* **60** Beiheft 1 (1982) 207.
8. W. SCHREYER, *Neues Jahrb. Miner. Abh.* **92** (1958) 147.
9. R. WIRTH and H. GLEITER, *Acta Metall.* **29** (1981) 1825.
10. M. HILLERT, *Met. Trans.* **3** (1972) 2729.
11. E. HORNBOGEN, *ibid.* **3** (1972) 2717.
12. C. ZENER, *Trans. AIME* **167** (1946) 550.
13. R. WIRTH, *Neues Jahrb. Miner. Abh.* **152** (1985) 101.
14. H. SCHUMANN, "Metallographie" (VEB Deutscher Verlag für Grundstoffindustrie, Leipzig, 1975) p. 58.
15. C. S. SMITH, *Trans. Amer. Soc. Met.* **45** (1953) 533.
16. D. A. CARMICHAEL, *Contrib. Mineral. Petrol.* **20** (1969) 244.
17. H. GLEITER and B. CHALMERS, *Progr. Mater. Sci.* **15** (1972) 139.
18. W. Q. KENNEDY, *Schweiz. mineralog. petrogr. Mitt.* **11** (1931) 76.
19. R. WIRTH, *Neues Jahrb. Miner. Abh.* **154** (1986) 193.
20. K. N. TU and D. TURNBULL, *Acta Metall.* **15** (1967) 369.
21. F. SPENCER, *Mineralog. Magazine* **26–7** (1945) 79.

Received 15 November 1985
and accepted 6 May 1986